PCCP

Physical Chemistry Chemical Physics

www.rsc.org/pccp

Volume 10 | Number 48 | 28 December 2008 | Pages 7189–7336

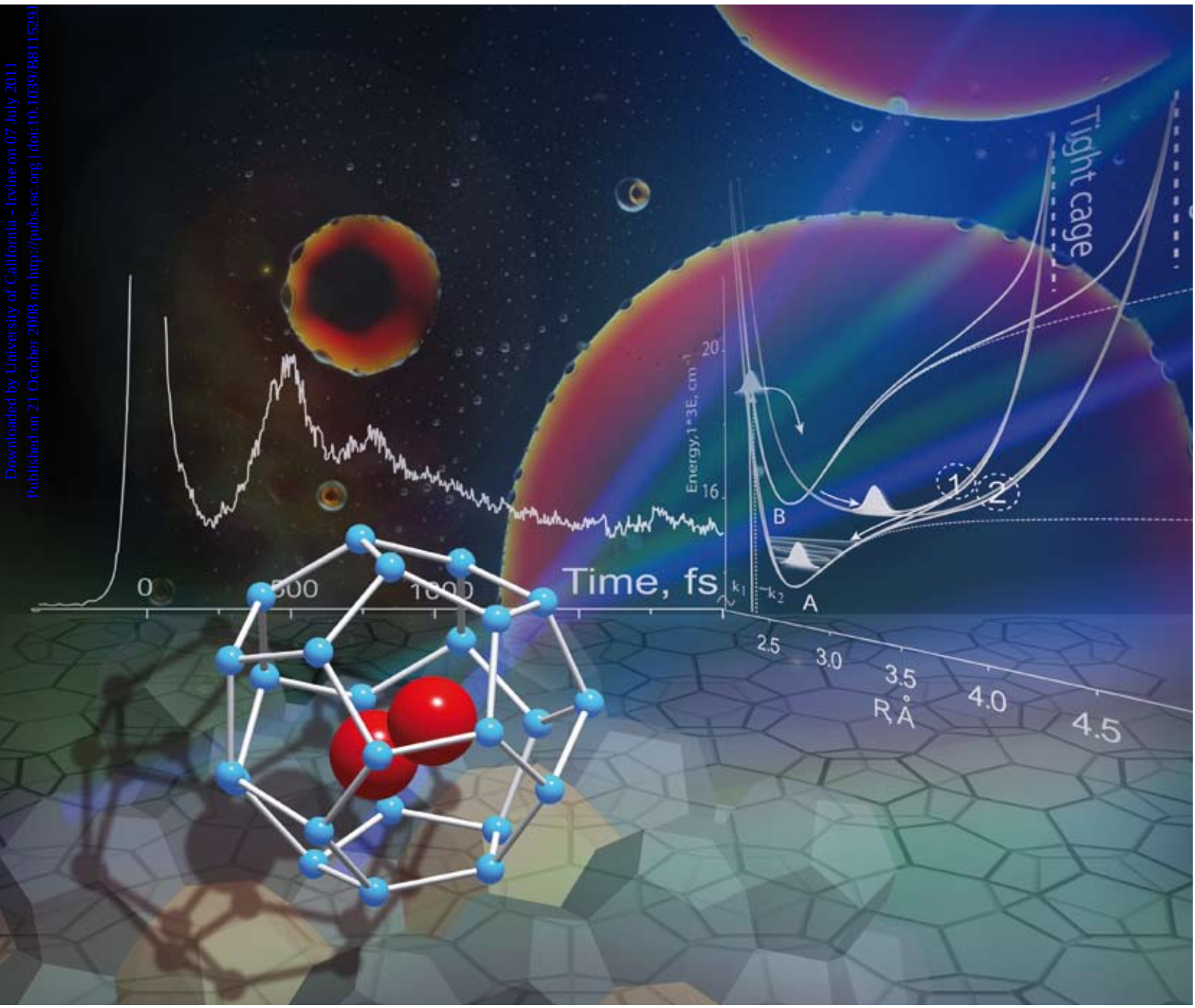

ISSN 1463-9076

Dynamical interrogation of the hydration cage of bromine in single crystal clathrate hydrates *versus* water

I. U. Goldschleger, G. Kerenskaya, V. Senekerimyan, K. C. Janda and V. A. Apkarian*

Received 8th July 2008, Accepted 17th September 2008
First published as an Advance Article on the web 21st October 2008
DOI: 10.1039/b811529j

We report transient grating measurements carried out on single crystals of bromine clathrate hydrates and on bromine dissolved in water. In all cases, excitation into the B-state of Br_2 leads to prompt predissociation, followed by cage-induced recombination on the A/A′ electronic surfaces. In liquid water, the vibrationally incoherent recombinant population peaks at $t = 1$ ps and decays with a time constant of 1.8 ps. In the hydrate crystals, the recombination is sufficiently impulsive to manifest coherent oscillations of the reformed bond. In tetragonal TS-I crystals, with the smaller cages, the recombination is fast, $t = 360$ fs, and the bond oscillation period is 240 fs. In cubic CS-II crystals, the recombination is slower, $t = 490$ fs, and the visibility of the vibrational coherence, which shows a period of 290 fs, is significantly reduced due to the larger cages and the looser fit around bromine. The mechanical cage effect is quantified in terms of the recombination time-distribution, the first three moments of which are associated with size, structural rigidity, and anelasticity of the cage. In the crystalline cages, the distribution is symmetric about the mean: mean time $t_m = 300$ fs, 400 fs and standard deviation $\sigma = 70$ fs, 100 fs, in TS-I and CS-II, respectively. The finding is consistent with the assignment of occupied cages: principally $5^{12}6^2$ polyhedra in TS-I and $5^{12}6^4$ polyhedra in CS-II. In liquid water, with diffuse cages, the distribution characterized by $t_m = 555$ fs and $\sigma = 400$ fs, is strongly skewed ($\gamma_1 = 1.88$) toward delayed recombination—the effective liquid phase hydration shell is larger than that in a hydrate phase, structurally disordered, and anelastic. Information about dipolar disorder, comparable in all three media, is extracted from electronic predissociation rates of the B-state, which is sensitive to the symmetry in the guest–host interaction.

Introduction

Solid hydrates of molecular halogens are among the first discovered clathrate hydrates, which are crystalline compounds consisting of guest molecules trapped in a lattice of polyhedral water cages.[1] Despite the importance of this class of inclusion crystals, many questions about their structure, energetics, and dynamics remain unanswered. In a set of recent works, we reported on the UV-Vis spectra of polycrystalline clathrates of bromine and iodine, to show that dramatic spectral changes accompany the different phases of liquid and solid halogen hydrates.[2,3] The spectral shifts could be rationalized by the local structure of the cages in which the dihalogens trap. Using resonant Raman and UV-visible absorption spectroscopy on carefully grown single crystals, we could demonstrate polymorphism in bromine hydrates with the identification of two distinct structures:[4,5] tetragonal TS-I,[6] in which Br_2 is expected to occupy $5^{12}6^2$ and $5^{12}6^3$ cages in a 4:1 ratio; and cubic CS-II,[7] in which Br_2 is expected to occupy the larger $5^{12}6^4$ cages. These assignments are indirect. The Raman spectra yield the vibrational frequency and anharmonicity of the guest molecule in its ground electronic state, in a well-accommodated host structure. The quantitative connection between spectral shifts and trapping site has not yet been made rigorously. Dynamical measurements on excited electronic states in which the molecule can be driven into large amplitude motion, provide a complementary method for probing the local cage, as we describe in the present study.

Starting with the seminal studies of Franck and Rabinowitch,[8] molecular halogens, and in particular molecular iodine, have been extensively used to interrogate the celebrated cage effect in liquids—the process that leads to geminate recombination of atoms upon photodissociation. Mechanisms and rates of geminate recombination on multiple electronic surfaces that correlate with the asymptotic limit of the separated atoms have been characterized through studies on ps and ns time scales.[9–11] With the advent of femtosecond lasers, the caging process could be monitored in the act, as first demonstrated in rare gas matrices[12,13] and in well-defined cages of SiO_2.[14] The common approach is to excite the molecular B-state (see Fig. 1), which undergoes solvent-induced predissociation, and to subsequently monitor the reformed molecular bond *via* suitable resonances.[15] Of the 18 states that arise from the recombination of $Br(^2P_{3/2}) + Br(^2P_{3/2})$, the $A(^3\Pi_{1u})$ and $A'(^3\Pi_{2u})$ are the deepest, nested excited states on which recombination takes place. They are collectively

Department of Chemistry, University of California, Irvine, CA 92697, USA. E-mail: aapkaria@uci.edu

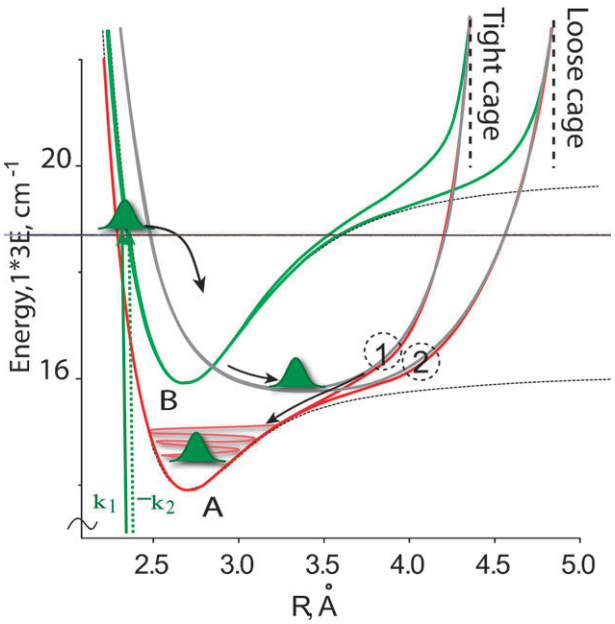

Fig. 1 A schematic diagram of potential energy surfaces and relaxation dynamics of caged Br_2. The dotted curves are the potentials of the bare molecule, which are modified by the repulsive walls of the cage when enclathrated. A population grating is prepared by 530 nm excitation on the electronically-excited B-state. In all cases, the B-state undergoes prompt predissociation, followed by electronic surface switching on the repulsive wall of the cage, and recombination on the A/A′ surfaces. The latter are represented by a single curve, but with two different repulsive walls arising from a "tight" (1), or "loose" (2) cage.

referred to as A/A′, and represented by the single curve in Fig. 1. Two important effects are probed in the process, the electronic effect of solvent-induced predissociation and the mechanical effect of cage-induced rebound. Both of these processes have been extensively studied in gas phase collisions as a function of pressure[16] and in clusters.[17,18] Electronic predissociation is swift in liquids: it occurs in ~250 fs for I_2(B) in liquid *n*-hexane.[19] Somewhat counter intuitive, in the denser rare gas solids the predissociation rates are reduced by an order of magnitude.[20,21] This electronic caging effect is understood in terms of the symmetry in guest–host interactions, which leads to cancellation of the solvent-induced electronic mixing.[22,23]

In principle, the mechanical cage effect could be used to gauge the size, structure and effective potentials experienced by the guest molecule. Thus, qualitatively, we understand that structural disorder in liquids and the soft fluid cage leads to dispersion in geminate recombination times. The consequence is the appearance of incoherent population on the ground (X-state) and shallow bound states that correlate with the asymptotic limit of the separated halogen atoms, of which A/A′ are the deepest.[16] In contrast, in low temperature rare gas matrices, which provide more rigid and structured cages, sudden recombination leads to coherent oscillations of the reformed bond on the A/A′ surfaces.[12] These general considerations hold for bromine as well, as detailed in a series of recent time-resolved studies.[24–26] A quantitative analysis of such measurements to characterize the nature of the interrogated cage—its effective size, structural order, and elasticity—has not been devised previously. Here, we propose the rebound time distribution as the characteristic dynamical probe of the cage, and we show how this can be directly extracted from the measurements. The utility of such probes in the investigation of clathrates, where all properties are related to cage structure, should be obvious. With this in mind, we have reported on transient grating (TG) measurements of Br_2 and I_2 in ice, to conclude that in the former the interrogated ensemble was that of molecules that impose clathrate structure locally; while in the latter, several trapping sites could be identified.[27,28]

Here, we report the first dynamical measurements on single crystal clathrate hydrates. While single crystals can be expected to provide a high level of structural order, peculiar to the water environment is dipolar disorder and dielectric fluctuations that control electronic mixing, and therefore control rates of predissociation. Although it is generally assumed that in clathrate hydrates the static electric field is vanishing in the vicinity of cage centers,[29] thermal fluctuations in guest–host configurations can be expected to destroy such symmetry. That indeed is what is observed in carefully prepared single crystals, as evidenced by the absence of any electronic caging, as we describe below. We should note that a significant challenge in carrying out these measurements has been the preparation of single crystals of high optical quality. As such, we start with a detailed description of the sample preparation.

Preparation of bromine hydrate crystals

We first prepare a polycrystalline bromine hydrate sample by flash freezing and subsequent refrigeration (+2 °C) a mixture of purified water (resistance 18 MΩ) and 99% pure bromine at constant mixing. Upon melting, the sample forms a supersaturated emulsion, which does not phase separate for a considerable time. The emulsion stays liquid down to −17 °C, allowing crystal growth by temperature control. The crystal growth and subsequent spectroscopic measurements are performed in a cell consisting of two windows separated by a 10 μm gap, using non-reactive fluorinated grease (Krytox®) as spacer and sealant. The top window is a standard microscope slide. The bottom window is 0.5 mm thick sapphire placed in contact with two Peltier elements (separated by 3 mm to allow the light to pass through the cell), which are in turn cooled by a water-cooled copper block. The apparatus allows control of temperature from +20 to −30 °C with a precision of 0.1 °C. The emulsion is transferred to the optical cell and quickly cooled to −20 °C to form seed crystals. Upon raising the temperature above 0 °C, the ice melts and reveals the seed crystals. These crystals are stable up to +5.8 °C, which corresponds to the melting point of bromine hydrate in the tetragonal crystalline form, TS-I. Careful cycling of the temperature around the hydrate melting point allows the isolation of few seed crystals in the optical path. These crystals are then allowed to grow for four days at +4.8 °C, to form optical quality crystals that fill the 10 μm gap between the windows, with dimensions up to 500 × 500 μm in the *x*–*y* plane. Type II bromine hydrate is grown in the same

experimental cell by dropping the temperature to −10 °C. As previously reported,[4] when the TS-I crystals are exposed to excess water at this temperature, a phase transition to the CS-II structure occurs on the surface of the TS-I crystals. After 24 h, optical quality single crystals of the CS-II hydrate grow in size, large enough (>100 μm) for the measurements.

The apparatus and methods of the two-color transient grating measurements that we implement here are identical to those already reported in the studies on halogen-doped ice.[27] Briefly, two coincident 70 fs pulses, resonant with the B ← X transition of Br_2 at 530 nm, are focused on the sample at an angle of 7° to create a population grating. A 70 fs pulse centered at 400 nm, resonant with the ion-pair states of the molecule, is used to read the grating as a function of delay between writing and reading. A single achromatic lens (focal length = 15 cm) is used to bring the three noncollinear beams into focus on the sample. The phase-matched signal propagating along the $\boldsymbol{k}_1 - \boldsymbol{k}_2 + \boldsymbol{k}_3$ direction (where 1, 2 refer to the visible write-beams, and 3 refers to the UV read beam) is then spatially filtered with an iris, spectrally filtered using a 1/4-meter monochromator, and collected using a cooled photomultiplier tube. A boxcar integrator is used to record and average the signal.

Results and analysis

In Fig. 2 we show the TG signal from a liquid Br_2/H_2O solution. Past $t = 0$, where the signal is saturated by the instantaneous nonresonant response of the medium, we see a build-up of population that peaks at $t = 1$ ps and decays exponentially. The build-up is subject to an induction period characteristic of sequential A → B → C kinetics. The fit shown in Fig. 2 is to the first-order sequential kinetic form:[30]

$$S(t)_{\text{water}} = [(\tau_1 e^{-t/\tau_1} - \tau_2 e^{-t/\tau_2})/(\tau_2 - \tau_1) + 1]e^{-t/\tau_3} \quad (1)$$

in which $\tau_3 = 1.8$ ps can be associated with the decay of population to the ground electronic state; while the signal build-up described inside the square paranthesis is characterized with very similar time constants, $\tau_1 = 285$ fs and $\tau_2 = 270$ fs. Evidently, the observation window is reached indirectly. Rather than observing the initially pumped B-state, the signal can be understood as the result of predissociation followed by electronic interconversion to the A/A′ surfaces. The conversion occurs on the repulsive cage wall where the electronic states that correlate with $Br(^2P_{3/2}) + Br(^2P_{3/2})$ coalesce and mix (see Fig. 1). The fit determines an upper bound for the predissociation time: it occurs promptly, in $t \leq \tau_2 = 270$ fs. Nevertheless, the recombination of the molecule is subject to large dispersion, as reflected by the delayed signal build-up. The dispersion in recombination times precludes coherence in the newly formed bond, as manifested by the absence of any modulation in the signal. We return to this consideration after noting the contrast in behavior in the crystals.

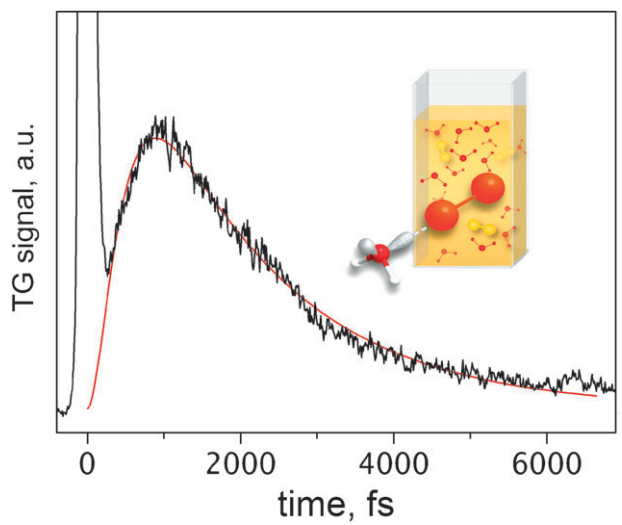

Fig. 2 Transient grating signal obtained for: bromine in liquid water (black trace) recorded at $T = 263$ K. The $t = 0$ signal is the response limited non-resonant background. The signal at positive time is due to the geminate recombination of Br_2 on the A/A′ surfaces. The decay of the signal is due to population transfer to the ground state. The red trace is the three-exponential fit, eqn (1), which accounts for build-up subject to induction and decay. In the inset we show the preferred binding geometry of a single water molecule to bromine. The binding is dominated by induction, by dipole-induced polarization of bromine, with the lone-pair of electrons on oxygen contacting Br_2 along the axial coordinate. Note, this geometry is not possible in the clathrate cage, where all electron-pairs of oxygen are occupied by intermolecular hydrogen bonds.

A set of measurements recorded on TS-I single crystals is shown in Fig. 3a. Now the recombination peak occurs at $t = 360$ fs, significantly earlier than in water. Moreover, the decay is modulated, indicating vibrational coherence characteristic of impulsive recombination. The observed period of oscillation, 240 fs, is close to the A-state harmonic period of the bare molecule: $\tau = 220$ fs (harmonic constant, $\omega_e = 153$ cm^{-1}, and anharmonicity, $\omega_e x_e = 2.7$ cm^{-1}).[31] Were we to assume gas-phase parameters, the observed period would correspond to motion near $v = 2$. We may therefore conclude that the probe window is located near the bottom of the potential, and that energy dissipation is rapid, *i.e.* the hydrate cage is efficient in accommodating the excess energy of the guest. After excitation to the B-state, the molecule predissociates, sheds ~4500 cm^{-1} of vibrational energy, and reaches the bottom of the A-state in $t < 0.5$ ps.

A set of measurements carried out in CS-II type single crystals is shown in Fig. 3b. The recombination peak occurs at 490 fs, significantly delayed relative to TS-I crystals, yet it occurs in nearly half the time it takes in liquid water. Past the well-defined peak, a shallow modulation can be seen over the decaying background, with an identifiable recursion at 780 fs. Were we to assume gas-phase parameters, the observed period of 290 fs would correspond to motion near $v = 7$. Alternatively, were we to assume that dissipation is as efficient as in the TS-I crystals, we would be lead to conclude that the effective potential of the molecule is perturbed—softened by attractive cage walls. The latter conclusion is consistent with the ground electronic state of the molecule based on Raman spectra, which show that the vibrational frequency in the CS-II crystals is down-shifted relative to that in TS-I.[4] Dramatic energy dissipation in the first bond excursion

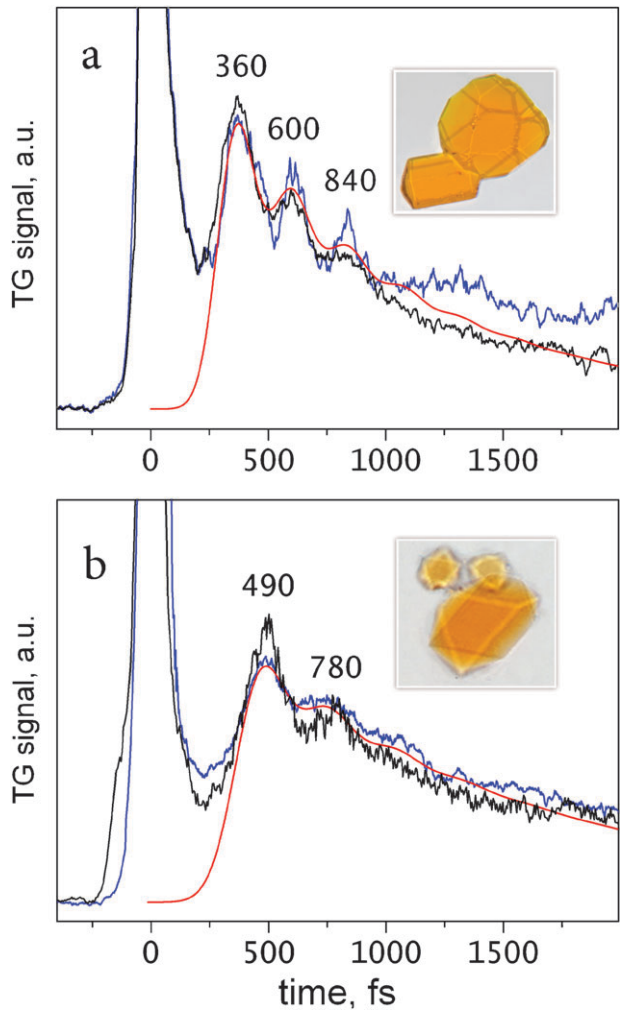

Fig. 3 Transient grating signals of bromine hydrate single crystals recorded at $T = 263$ K: (a) tetragonal TS-I structure, in which 80% of the bromine molecules occupy $5^{12}6^2$ cages. (b) CS-II clathrate hydrate single crystal, in which bromine occupies $5^{12}6^4$ cages. The different traces correspond to measurements made on different spots in the same crystal. The saturated signal at $t = 0$ arises from the nonresonant scattering in both sample and cell windows. The delayed recovery of the signal, is due to cage-induced recombination on the A/A′ surfaces after predissociation out of the B-state. In TS-I the recombinant population peaks at $t = 360$ fs, and shows vibrational coherence with a period of 240 fs. In CS-II, the recombination peak occurs at $t = 490$ fs, with much fainter vibrational coherence, with a period of 290 fs. The red curves are the fits to eqn (3), with extracted parameters collected in Table 1.

accompanied by a large change of period between first and second cycles of motion, is typical of caged molecules prepared above their dissociation limit, as catalogued for A/A′,[12,13] B,[21] and cage-bound states[32] of iodine in rare gas matrices. In the hydrate cages, CS-II or TS-I, we observe such efficient relaxation to extend down to the bottom of the potential. This, in part, can be attributed to the temperature at which the measurements are made: $T = 265$ K, which is comparable to vibrational spacings ($\hbar\omega_e/kT = 1.2$). As such, efficient vibrational dissipation and dephasing is to be expected.

The trend of the delay in recombination time and the extent of vibrational coherence in the newly formed bond in proceeding from TS-I to CS-II crystals to water can be associated with the size and structural rigidity of the hydration cage. In TS-I crystals 80% of the Br_2 molecules are expected to trap in the tight-fit $5^{12}6^2$ cages while 20% are trapped in $5^{12}6^3$ cages. In CS-II, the molecule is trapped in the looser $5^{12}6^4$ cage. Despite the presence of two different sites in TS-I, and only one in CS-II, the vibrational coherence is better defined in the former—the signal is more deeply modulated. An essential condition for observing vibrational coherence in a newly formed bond is that the dispersion in recombination times is smaller than the molecular vibrational period. This suggests the impulsiveness of the induced recombination as the characteristic mechanics of the cage effect—an attribute that can be quantitatively extracted from the data. Thus, for sudden recombination described as a delta impulse in time, $I(t) = \delta[t - t_0]$, the expected signal is the transfer function:

$$T(t) = \sin(2\pi t/\tau)e^{-t/\tau_v} + e^{-t/\tau_p} \quad (2)$$

which describes damped vibrations with period τ, coherence decay τ_v due to vibrational dissipation and dephasing; and population decay τ_p. For an arbitrary impulse, the linear response is the convolution of impulse and transfer function:

$$R(t) = \int I(t - t')T(t)dt' \quad (3)$$

Using eqn (2), the clathrate data can be adequately reproduced with impulse functions that are Gaussian in time:

$$I(t) = \frac{1}{\sigma\sqrt{2\pi}}\exp\left[-\frac{(t - t_m)^2}{2\sigma^2}\right] \quad (4)$$

in which t_m and σ represent the mean and standard deviation in cage induced recombination times. The parameters extracted from the fits shown in Fig. 3a and b are collected in Table 1. A direct comparison with the cage mechanics in water is afforded by identifying the impulse function in water as the rate of population build-up in (1):

$$I(t)_{\text{water}} = \frac{1}{\tau_2 - \tau_1}(e^{-t/\tau_2} - e^{-t/\tau_1}) \quad (5)$$

with mean:

$$t_m = \int_0^\infty tI(t)_{\text{water}}dt = \tau_1 + \tau_2 \quad (6)$$

standard deviation:

$$\sigma = \left[\int_0^\infty (t - t_m)^2 I(t)_{\text{water}}dt\right]^{1/2} = \sqrt{\tau_1^2 + \tau_2^2} \quad (7)$$

and standardized skewness:

$$\gamma_1 = \frac{1}{\sigma^3}\int_0^\infty (t - t_m)^3 I(t)_{\text{water}}dt = \frac{2(\tau_1^3 + \tau_2^3)}{\sigma^3} \quad (8)$$

The normalized impulse functions, which represent the distribution of cage-induced recombination times, are shown in Fig. 4. The observed trends lend themselves to simple mechanistic interpretations, diagnostic of the structure and nature of the local cage.

Table 1 Characterization of caging dynamics

	Impulse function		Population decay	Coherence decay	Vibrational period
	t_m/fs	σ/fs	τ_p/ps	τ_v/fs	τ/fs
TS-I	300	70	0.9	300	240
CS-II	400	100	1.3	300	290
Water	555	400	1.8		

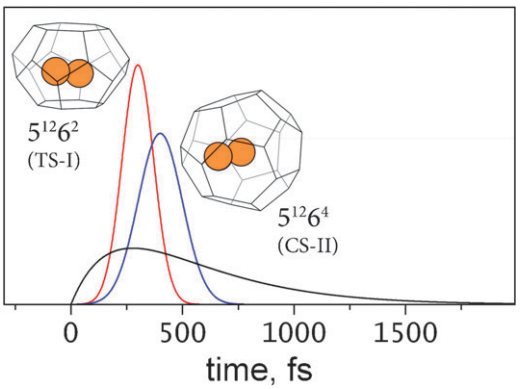

Fig. 4 The normalized impulse functions, which describe the distribution of cage-induced recombination times in TS-I (red) and CS-II (blue) single crystals and in water (black), are shown. The impulse functions are symmetric in time in the solid cages, with mean and variance (see Table 1) that correlate directly with the depicted cage size and guest-cage configuration distribution (looseness of fit). The impulse function in water is significantly delayed and broader. The more important distinction of the anelastic fluid cage is the skewed impulse function with its long tail of delayed geminate recombination.

The mean time of rebound, t_m = 300, 400, 555 fs in TS-I and CS-II and water, can be associated with the effective size of the cage. It clearly distinguishes the two crystals, and assuming the same mechanics, it suggests that the effective size of the cage in liquid water is larger than either. The latter suggestion is nontrivial. Through neutron diffraction studies and analysis, it has been shown that the hydration shell around methane in the liquid water is 1 Å tighter than in the crystalline hydrate.[33] Both the hydration number in the first shell of methane and the orientation of water molecules are different in the two phases. That the hydration structure around bromine is quite different in the two phases, is demonstrated by the dramatic spectral shift in UV-Vis spectra, and explained based on oxygen-bonding of water to the polarizable bromine in the liquid phase (see inset to Fig. 1), and the unavailability of such binding in the clathrate hydrate solids (see structures in Fig. 4).[27] That as a result, the hydration cage of polarizable bromine is larger in the liquid phase than in the solid, would not be entirely surprising. A reservation in this consideration is the distinction in the mechanics of rebound from a solid cage *versus* a liquid shell. Both elasticity and structural integrity of the cages are quite different, and as such the association of the delay in recombination with size alone is questionable.

The dispersion in rebound times, σ = 70, 100, 400 fs, would be expected to be controlled by the distribution in cage-molecule configurations—a measure of the looseness of the fit. Consistent with this interpretation the distribution broadens dramatically in water, in which the cage structures are transient and diffuse. The width of the distribution distinguishes the two cage structures (shown in Fig. 4), and recognizes that the fit is looser in the $5^{12}6^4$ cages of the CS-II lattice. Finally, the symmetry of the distribution is informative as a measure of the cage elasticity. The strongly skewed (γ_1 = 1.88) distribution in water, with a long delayed recombination tail that is limited by the observation window, indicates a non compliant cage response characteristic of anelasticity (response in which strain lags stress). With the same consideration, the observed symmetry of the distribution function in the solid state may be associated with the elasticity of the cage response. In this regard, the two cages are similar.

What pertains to the cage-induced electronic perturbations is contained in the observed rates of curve crossings. We see a definite trend in the population decay out of the A/A′ states: t_p = 0.9, 1.3, and 1.8 ps, in TS-I, CS-II and water, respectively. In all cases the lifetimes are significantly shortened to quench emission from these states—emissions that are prominent in cryogenic rare-gas solids.[34–36] Assuming fast equilibration between the A($^3\Pi_{1u}$) and A′($^3\Pi_{2u}$) states, conversion to the ($^1\Sigma_g$)-ground state requires electric field anisotropy to induce $u \leftrightarrow g$ mixing, and electronic torque to change angular momentum. It would seem that these perturbations are more effective in the tighter cages, when the molecule is forced into close contact with the cage walls. With regard to the predissociation of the B-state, it is remarkable that in all cases it proceeds with near unit probability in $t < 250$ fs. There is no evidence of electronic caging. This is to be contrasted with the measurements of bromine trapped in nominally cubic ice, in which coherent vibrations of a population trapped below v = 3 of the B-state could be monitored for several ps.[27] Indeed, through careful analysis of Franck–Condon intensities, the lowest crossing on the B-state has been identified to occur near v = 4 in solid Ar, and assigned to the crossing between B($^3\Pi_{0u}$) and C($^1\Pi_{1u}$).[26] There, as in ice at T = 120 K,[27] vibronic coherence trapped below the crossing can be observed for several picoseconds. The observed enhancement of the predissociation probability to unity in the present, when contrasted with the ice data, singles out temperature as the principle difference. The thermal effect that can be active on the timescale of a half-period of motion is structural disorder. Given the characters of the electronic states involved (same parity, different angular momentum, different spin multiplicity), the enhanced coupling cannot be trivially explained. Minimally multipolar field gradients, which presumably arise from thermal fluctuations of the polar lattice, would be required. Also, the optically silent B′($^3\Pi_{0u}^-$) state may contribute to predissociation, as invoked in the analysis of fluorescence intensities in Ar matrices.[36] Temperature-dependent

measurements could confirm that thermally induced dipolar disorder is probed by the electronic predissociation of the molecule. However, the present method of sample preparation did not allow significant temperature variation—the crystals crack and scatter light, precluding TG measurements.

Conclusions

We reported the first-time domain measurements of molecular photodynamics in single crystals of clathrate hydrates. The dynamical measurements in which the molecule is driven into large amplitude motion clearly demonstrate enclathration of Br_2 in two distinct cages, in the two crystalline structures that were recently identified through Raman and UV-visible absorption spectroscopy.[4] In the larger cages of the CS-II crystal, recombination times are delayed and are subject to a broader dispersion than in the TS-I crystals, in which the tighter confinement of the molecule translates into faster and more sudden recombination. This is recognized by the extent of the vibrational coherence of the reformed bond, and quantified using a simple model that characterizes the mechanics of caging through the time-distribution of recombination, with moments of the distribution being associated with size, structural order, and elasticity of the local cage. A more rigorous connection awaits molecular dynamics simulations of the system.

In both crystals and in water the predissociation of the B-state is completed within one vibrational period, suggesting that the dielectric disorder sampled by the molecule in the two phases is similar. These results are to be contrasted with our prior observations of Br_2 and I_2 doped ice. There, in the case of Br_2, a fully modulated vibronic coherence trapped on the B-state is observed, below the B/C curve crossing (below $v = 3$). Based on the persistence of the coherence in ice the molecule appears to be mechanically decoupled from the lattice. Based on the slow predissociation and sharply defined charge transfer resonances it is inferred that the molecule is electrically insulated from the lattice.[27,37] These contrasts with the present single-crystal measurements reinforce the conclusion that the ensemble monitored in ice consists of molecules trapped in perfect clathrate cages. Moreover, we are lead to conclude that the single crystals near 0 °C are subject to significant dipolar disorder. In the case of I_2, a variety of trapping sites is observed in ice, with varying predissociation rates.[28] Notably, in high symmetry sites where electronic caging is complete and vibrational coherence on the B-state can be tracked, the cages are mechanically non-compliant—they expand upon impact and the molecule follows the cage expansion adiabatically. Despite its symmetry, the hydration shell around I_2 remains an incomplete cage in ice. This is consistent with fact that I_2 alone does not form clathrate hydrate crystals.

More generally, we have provided an analysis of caging dynamics, which can be broadly implemented to characterize the local structure of trapped molecules. The method is particularly valuable in cases where long-range structural order may not be present, such as in inclusion solids where the guest may be a dilute impurity, as already demonstrated in the studies in ice.

Acknowledgements

This work was supported by the National Science Foundation Grant No. CHE-0404743. VAA gratefully acknowledges the insightful discussions with N. Halberstadt during the course of writing of this manuscript, and her earlier contributions to the shaping of the concept of electronic caging.

References

1 E. D. Sloan, Jr, *Clathrate Hydrates of Natural Gases*, Marcel Dekker, New York, 1998.
2 G. Kerenskaya, I. U. Goldschleger, V. A. Apkarian and K. C. Janda, *J. Phys. Chem. A*, 2006, **110**, 13792.
3 G. Kerenskaya, I. U. Goldschleger, V. A. Apkarian and K. C. Janda, *J. Phys. Chem. A*, 2007, **111**, 10969.
4 I. U. Goldschleger, G. Kerenskaya, K. C. Janda and V. A. Apkarian, *J. Phys. Chem. A*, 2008, **112**, 787.
5 UV-Vis absorption spectra of TS-I and CS-II single crystals are distinguishable by a relative shift of 440 cm^{-1} in their absorption maxima. K. C. Janda, G. Kerenskaya, I. U. Goldschleger and V. A. Apkarian, *Proceedings of the 6th International Conference on Gas Hydrates*, 2008.
6 K. A. Udachin, G. D. Enright, C. I. Ratcliffe and J. A. Ripmeester, *J. Am. Chem. Soc.*, 1997, **119**, 11481.
7 T. C. W. Mak and R. K. McMullan, *J. Chem. Phys.*, 1965, **62**, 2732.
8 J. Frank and E. Rabinowitch, *Trans. Faraday Soc.*, 1934, **30**, 120.
9 H. Hippler, V. Schubert and J. Troe, *J. Chem. Phys.*, 1984, **81**, 3941.
10 A. L. Harris, J. K. Brown and C. B. Harris, *Annu. Rev. Phys. Chem.*, 1988, **39**, 341.
11 N. A. Abul-Haj and D. F. Kelley, *J. Chem. Phys.*, 1986, **84**, 1335.
12 R. Zadoyan, Z. Li, C. C. Martens and V. A. Apkarian, *J. Chem. Phys.*, 1994, **101**, 6648.
13 R. Zadoyan, Z. Li, P. Ashjian, C. C. Martens and V. A. Apkarian, *Chem. Phys. Lett.*, 1994, **218**, 504.
14 G. Flachenecker, V. A. Ermoshin, V. Engel, R. Neder, G. Wirnsberger and A. Materny, *Phys. Chem. Chem. Phys.*, 2003, **5**, 865.
15 For the relevant electronic states of Br_2 in the gas phase, see: J. Tellinghuisen, *J. Chem. Phys.*, 2003, **118**, 1573.
16 C. Lienau and A. H. Zewail, *J. Phys. Chem.*, 1996, **100**, 18629.
17 Q. Liu, J.-K. Wang and A. H. Zewail, *Nature*, 1993, **364**, 427.
18 C. Wan, M. Gupta, J. S. Baskin, Z. H. Kim and A. H. Zewail, *J. Chem. Phys.*, 1997, **106**, 4353.
19 N. F. Scherer, D. M. Jonas and G. R. Fleming, *J. Chem. Phys.*, 1993, **99**, 153.
20 R. Zadoyan, M. Sterling and V. A. Apkarian, *J. Chem. Soc., Faraday Trans.*, 1996, **92**, 1821.
21 M. Gühr, M. Bargheer, P. Dietrich and N. Schwentner, *J. Phys. Chem. A*, 2002, **106**, 12002.
22 R. Zadoyan, M. Sterling, M. Ovchinnikov and V. A. Apkarian, *J. Chem. Phys.*, 1997, **107**, 8446.
23 V. S. Batista and D. F. Coker, *J. Chem. Phys.*, 1997, **106**, 6923.
24 M. Bargheer, M. Gühr and N. Schwentner, *Isr. J. Chem.*, 2004, **44**, 9.
25 M. Gühr and N. Schwentner, *Phys. Chem. Chem. Phys.*, 2005, **7**, 3143.
26 H. Ibrahim, M. Gühr and N. Schwentner, *J. Chem. Phys.*, 2008, **128**, 064504.
27 I. U. Goldschleger, V. Senekerimyan, M. S. Krage, H. Seferyan, K. C. Janda and V. A. Apkarian, *J. Chem. Phys.*, 2006, **124**, 204507.
28 V. Senekerimyan, I. U. Goldschleger and V. A. Apkarian, *J. Chem. Phys.*, 2007, **127**, 2145111.
29 D. W. Davidson, *Can. J. Chem.*, 1971, **49**, 1224.
30 See for example, H. Eyring, S. H. Lin and S. M. Lin, *Basic Chemical Kinetics*, Wiley Interscience, New York, 1980.
31 J. A. Coxon, *J. Mol. Spectrosc.*, 1972, **41**, 548.
32 Z. Bihary, R. Zadoyan, M. Karavitis and V. A. Apkarian, *J. Chem. Phys.*, 2004, **120**, 16.

33 C. A. Koh, R. P. Wisbey, X. Wu, R. E. Westacott and A. K. Soper, *J. Chem. Phys.*, 2000, **113**, 6390.
34 E. Bondybey and C. Fletcher, *J. Chem. Phys.*, 1976, **64**, 3615; J. Langen, K.-P. Lodemann and U. Schurath, *Chem. Phys.*, 1987, **112**, 393.
35 J.-P. Nicolai and M. C. Heaven, *J. Chem. Phys.*, 1985, **83**, 6538.
36 J. Langen, K.-P. Lodemann and U. Schurath, *Chem. Phys.*, 1987, **112**, 393.
37 I. U. Goldschleger, V. Senekerimyan and V. A. Apkarian, *J. Phys. Chem.*, 2008, submitted.

